Spaceborne Doppler Atmospheric Radar: an overview for measuring atmospheric dynamics

Simone Tanelli
Jet Propulsion Laboratory, California Institute of Technology, Pasadena CA, USA
E-mail: simone.tanelli@jpl.nasa.gov ; Tel: +1-818-354-0195; Fax: +1-818-393-6440

Knowledge of the global distribution of the vertical velocity of precipitation and cloud constituents is important in estimating latent heat fluxes, and therefore in the study of energy transportation in the atmosphere, the climate and weather. Such knowledge can only be directly acquired with the use of spaceborne Doppler Atmospheric Radars (DAR). A Doppler Atmospheric Radar (DAR) is a spaceborne coherent radar designed to detect hydrometeors and their motion. Two main sub-categories of atmospheric radars can be roughly discriminated by their operating frequency, the Precipitation Radars (PR, at 35 GHz or lower) and Cloud Profiling Radars (CPR, at 35 GHz or higher).
The use of coherent systems is well established in the ground and airborne weather radar community and the advantages brought by the Doppler capability (i.e., direct measurement of the speed of the hydrometeors relative to the radar) are widely recognized.
Although, the use of Doppler systems from space to measure atmospheric targets is hindered by the high orbiting velocity of the radar (which introduces issues and effects otherwise negligible for slower platforms), the average vertical velocity can be measured to acceptable accuracy levels. Such result can be obtained only by appropriate selection of radar parameters and data processing algorithms, and by recognizing some general trade-off considerations in the radar system design.

1. Radar Advantages & TRMM's Heritage

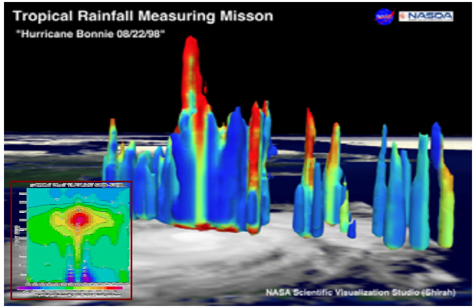

- Penetrate all precipitating and non-precipitating clouds relative to standard GOES cloud imagery
- Characterize precipitating system structure even in the presence of upper-level clouds
- Enable 3-dimensional profiling of critical parameters and dynamics which control and/or determine the formation and evolution of atmospheric events
  - Rain intensity
  - Vertical motion
  - Cloud process
  - Latent heat release
- Provide such data for NWPs improved forecast and understanding hurricane and storm dynamics

- Assimilation of TRMM precipitation data in global models
  - Improves climate analysis
  - Improves storm track forecast
  - Improves precipitation forecast

5 day forecast of Bonnie storm track

Red: best track (NOAA HRD)
Green: forecast from analysis w/o TRMM data
Blue: forecast from analysis with TRMM data

(From NASA/GSFC Data Assimilation Office (DAO); courtesy of Arthur Hou)

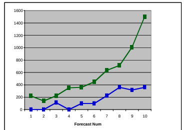

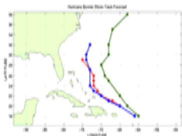

Latent Heating for Hurricane Bonnie from Vertical Derivative of Rain Mass Flux
Droplet Fall Velocities Derived from TRMM Combined Radar-Radiometer Algorithm 2b31
(S. Yang, Z. Haddad, & E. Smith)

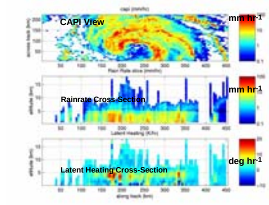

2. Why Doppler?

Goal	Potential of Doppler	Alternative spaceborne observing systems & methods	Contribution to Weather and Climate knowledge
Measurement of Vertical Air Motion and Characterization of Convection	**Extreme**	None in precipitation Š Potential use of lidar in clear air	- Improvement in GCM's skills by assimilating vertical velocity - Understanding of precipitation processes and dynamics on a global scale - Improvement in the characterization of convection (vertical profiling and temporal evolution) - Improvement of global databases for characterizing convection in models
Hydrometeor Classification	Moderate	Radiometers - *limited vertical resolution.* Non-Doppler multi-frequency radars - *performances to be verified.*	- Cloud microphysics - Task CS
Estimation of Precipitation and DSD parameters	High in stratiform Moderate in convection	Multiparametric approaches (multifrequency, combined radar/radiometer) - *limted accuracy and/or vertical resolution*	- Improvement in rainfall rate estimates for assimilation in GCM's
Convective/Stratiform Classification	Moderate	Non-Doppler Radar - *acceptable performances over the tropics(TRMM) - to be verified on a global scale (GPM)*	- Improvement in Latent Heating global maps - Improvement in radiation budget studies - Improvement in rainfall rate estimates
Latent Heat	High	Multiparametric approaches (multifrequency, radar/radiometer) - *good in estimating maximum, unreliable performances in vertical profiling*	- Improvement in Latent Heating vertical profiling for assimilation in atmospheric models

Estimation of Rainfall Parameters

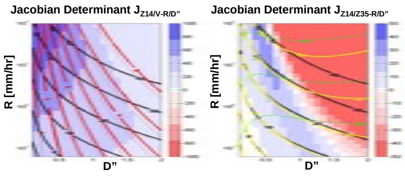

Color
- Reflectivity 14 GHz [dBZ]
- Mean Doppler velocity [m/s]
- Reflectivity 35 GHz [dBZ]
- Specific Attenuation 35 GHz [dB/km]

Linestyle
- s" = 0.38
- s" = 0.34
- s" = 0.42

Latent Heat in Precipitating Systems

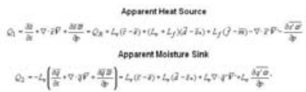

- **Latent Heat Absorption/Release** due to the water phase changes is one of major contributors to the overall heating.
- **Stratiform Precipitation**: heating in the upper troposphere and cooling in the lower troposphere. Vertical profiles are quite consistent over the globe (aside from the altitude of the ŌsignŌ change which is dependent on the altitude of the melting layer)
- **Convective Cells**: Heating and cooling are determined by the presence and magnitude of updrafts and downdrafts. Vertical profiles of latent heating differ significantly from stratiform precipitation and are also quite different for different regions, seasons and even within the diurnal cycle.
- **Surface Rainfall Rate**: assuming no horizontal advection, the surface rainfall rate corresponds to the integral (column) amount of condensated liquid water and can therefore be used to estimate the integral latent heat released.
- **Refer to**: Yanai et al. 1973, Houze 1982, Houze 1989, Tao et al. 2001

ACKNOWLEDGEMENT

The research described in this paper was carried out by the Jet Propulsion Laboratory, California Institute of Technology, under contract with the National Aeronautics and Space Administration.

3. Airborne and Spaceborne Doppler Radars

JPL Airborne Precipitation Radars

The 3-D high resolution datasets obtained by the two JPL airborne radars are the primary dataset used in this investigation.

ARMAR: Ku-band, dual-pol, Doppler, scanning radar
APR-2: See table below and diagram to the right

Parameters	Ku-band	Ka-band
Frequency	13.4 GHz	35.6 GHz
Polarization	HH, HV	HH, HV
Antenna effective diameter	0.4 m	0.14 m
Antenna gain	34 dBi	33 dBi
Antenna sidelobe	-30 dB	-30 dB
Antenna scan angle	±25Þ	±25Þ
Polarization isolation	-25 dB	-17dB
Peak power	200 W	100 W
Bandwidth	4 MHz	4 MHz
Pulse width	10 - 40 µs	10 - 40 µs
Pulse Repetition Frequency	5 kHz	5 kHz
Vertical resolution	37 m	37 m
Horiz resolution:		
At 9 km (30,000 ft) altitude	600 m	600 m
At 6 km (20,000 ft) altitude	400 m	400 m
Ground Swath		
At 9 km altitude	8.5 km	8.5 km
At 6 km altitude	5.6 km	5.6 km
Sensitivity:		
At 7 km range	5 dBZ	5 dBZ
Doppler precision	0.5 m/s	1 m/s

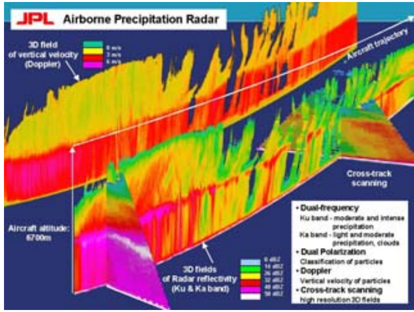

Dual-Frequency Doppler Spaceborne Radar for Hurricane Monitoring (Dr. Eastwood Im)

- 14 GHz (Ku-band) and 35 GHz (Ka-band) dual-frequency radar
- Deployable antenna reflector with matched beams (4 m x 4.3 m x 3 panels)
  - Horizontal resolution: 2.5 km @ h=380 km
- Wide-swath coverage using adaptive scanning: ± 30˚scan, ~440 km swath @ h=380 km
- Simultaneous HH and HV polarization
- On-board, real-time pulse compression: 250 m vertical resolution
- Transmit peak power required: 640 W @ 14 GHz; 280 W @ 35 GHz
- Enhanced minimum detectable Z: 6 dBZ @ 14 GHz; 2 dBZ @ 35 GHz
- 14-GHz vertical Doppler meas. @ 1 m/s precision
- On-board processing: Doppler, pulse averaging

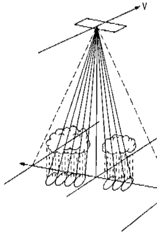

Nexrad-In-Space (Dr. Eastwood Im)

- Monitoring time evolution of rain & cloud from GEO (alt. = 36,000 km)
- 35-GHz, 4˚ spiral scanning radar to cover 5300-km diameter earth disk (equivalent to coverage of 48˚ latitude and 48˚ longitude)
- Deployable spherical aperture antenna to obtain 12 to 14 km horizontal resolution
- Innovative antenna scan strategy:
  - 1 transmit feed and 1 receive feed with fixed spacing to compensate for pulse delay
  - Scan by motion of 2 feeds on spiral path
    - Advantage over 2-D electronic scan, which requires millions of phase shifters
    - Advantage over mechanical rotation of entire antenna, which creates unacceptable torque
    - Advantage over S/C rotation, which requires custom-made, usually very expensive S/C
- Vertical resolution of 300 m using pulse compression
- Rain detection sensitivity: ~ 5 dBZ (after 100 sample averaging)
  - ~12 dB more sensitive than the TRMM radar
- Vertical Doppler profile measurements with 0.3 m/s precision
- One 3-D full-scan image once per hour
- Real-time processing to reduce downlink data volume/rate

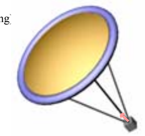

EarthCARE (ESA/NASDA Earth Explorer selection '04)

- 94 GHz (W-band) radar
- Vertical Doppler meas.

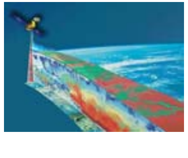

4. DAR performance in Doppler measurements

The natural Doppler velocity spectrum of rainfall

- **Shape**: approximately Gaussian.
- **Spectral width σ_R**: in the 1-5 m/s range, depending mainly on DSD, turbulence and wind speed.
- **Mean vertical velocity**: depends mainly on the DSD and vertical component of wind (up- and down-drafts).
- Received complex signal: zero-mean Gaussian.
- Signal power fluctuation: negative exponential distribution.

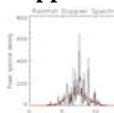

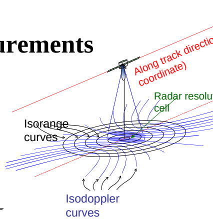

Radar **observed Doppler velocity** is the radial component of the relative motion of the target (raindrops) in an elementary volume at coordinates *(r, θ, φ)* with respect to the radar:

$$v_r = (v_x - v_s)\cdot\sin\theta\cos\phi + v_y\cdot\sin\theta\sin\phi + v_z\cdot\cos\theta$$

where v_x, v_y, and v_z (i.e., $\mathbf{v} = [v_x, v_y, v_z]$) are the particle velocity components in the along track, cross track and vertical direction respectively. V_S is the satellite speed (around 7 km/s)

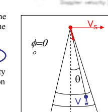

A pulsed Radar calculates the moments of the Doppler spectrum from sequence of M complex radar samples $\{\tilde{s}_n\}$ received from each resolution cell

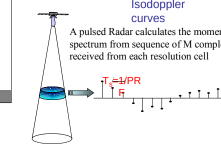

When the Doppler broadening induced by the satellite dominates over the width of the rainfall spectrum σ_R, the normalized Doppler spectral width is inversely proportional to antenna size.

The aliased portion of the Power spectrum introduces a bias and increases the variance of estimates.

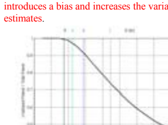

Normalized spectral widths

for different radar configurations (Op.Freq.,Antenna Size D (m) & PRF (Hz)) and 3 turbulence regimes (σ_R=1 m/s mild, σ_R=3 m/s moderate, σ_R=5 m/s extreme)

Ku band (13.6 GHz)

σ_R	D	2	3	4	5	6	10
	θ_{3dB} / PRF	.76	.51	.38	.30	.25	.15
1	5000	.50	.34	.25	.20	.17	.10
	6000	.42	.28	.21	.17	.14	.09
	7000	.36	.24	.18	.14	.12	.07
	8000	.32	.21	.16	.13	.11	.06
3	5000	.51	.34	.26	.21	.18	.11
	6000	.42	.28	.22	.17	.15	.10
	7000	.36	.24	.18	.15	.13	.08
	8000	.32	.21	.16	.13	.11	.07
5	5000	.51	.35	.27	.22	.19	.14
	6000	.43	.29	.22	.18	.16	.11
	7000	.37	.25	.19	.16	.14	.10
	8000	.32	.22	.17	.14	.12	.08

Ka band (35 GHz)

σ_R	D	2	3	4	5	6	10
	θ_{3dB} / PRF	.29	.20	.15	.12	.10	.06
1	5000	.51	.34	.26	.21	.17	.11
	6000	.42	.28	.21	.17	.15	.09
	7000	.36	.24	.18	.15	.12	.08
	8000	.32	.21	.16	.13	.11	.07
3	5000	.52	.36	.29	.25	.22	.17
	6000	.44	.30	.24	.20	.18	.14
	7000	.37	.26	.21	.18	.16	.12
	8000	.33	.23	.18	.15	.14	.11
5	5000	.56	.41	.34	.31	.29	.25
	6000	.46	.34	.29	.26	.24	.21
	7000	.40	.29	.25	.22	.21	.18
	8000	.35	.26	.21	.19	.18	.16

W band (94 GHz)

σ_R	D	2	3	4	5	6	10
	θ_{3dB} / PRF	.11	.07	.05	.04	.04	.02
1	5000	.52	.36	.28	.24	.21	.16
	6000	.43	.30	.23	.20	.17	.13
	7000	.37	.26	.20	.17	.15	.11
	8000	.32	.22	.18	.15	.13	.10
3	5000	.63	.50	.45	.43	.41	.39
	6000	.52	.42	.38	.36	.34	.32
	7000	.45	.36	.32	.30	.29	.28
	8000	.39	.32	.28	.27	.26	.24
5	5000	.80	.71	.68	.66	.65	.63
	6000	.67	.59	.56	.55	.54	.53
	7000	.57	.51	.48	.47	.46	.45
	8000	.50	.44	.42	.41	.41	.40

VERY BROAD	Pulses are uncorrelated, Doppler spectrum is almost white
BROAD	Pulses are almost uncorrelated, Doppler ambiguity reduces the unbiased Doppler unambiguous range by > 40%
INTERMEDIATE	Pulses are moderately correlated, Doppler ambiguity reduces the effective Doppler unambiguous range by 5-40%
NARROW	All results obtained for ground based and airborne Doppler radars are valid

Range (km)/Doppler (m/s) ambiguity trade-offs

All Freq.	Freq / PRF	13.6 GHz	35 GHz	94 GHz
30.0	5000	27.6	10.7	4.0
25.0	6000	33.1	12.9	4.8
21.4	7000	38.6	15.0	5.6
18.7	8000	44.1	17.1	6.4

Pulse Pair (PP) technique (one-lag correlation)

$$\hat v^{PP} = -\frac{\lambda}{2}\frac{1}{2\pi T_S}\arg\left(\frac{1}{M-1}\sum_{n=-(M-1)/2}^{(M-1)/2-1}\tilde{s}_n^*\tilde{s}_{n+1}\right)$$

DFT technique (spectral estimation)

$$\hat v^{DFT} = -\frac{\lambda}{2MT_S}\left\{\hat m' + \frac{1}{(S_P+S_N)-\hat S_N}\sum_{m=\hat m'-M/2}^{\hat m'+M/2}(m-\hat m')\cdot\left[\left(P_{mod_M(m)}+N_{mod_M(m)}\right)-\hat N_{mod_M(m)}\right]\right\}$$

DFT power spectrum of signal; DFT power spectrum of noise; Noise power; Signal power; Estimated noise power; Estimated power spectrum of noise

Max Rng (Km)	Freq / PRF	13.6 GHz	35 GHz	94 GHz
30.0	5000	27.6	10.7	4.0
25.0	6000	33.1	12.9	4.8
21.4	7000	38.6	15.0	5.6
18.7	8000	44.1	17.1	6.4

- PP is best performing for $w_N < 0.1$
- PP is affected by bias for $|f_N| > 0.5 - 4\,(w_N)^2$
- PP is affected by spectrum asymmetry
- PP is computationally more efficient

- DFT-2 is best performing for $0.1 < w_N < 0.2$
- DFT-2 is affected by bias for $|f_N| > 0.5 - 5\,(w_N)^2$
- DFT-2 is more affected by low SNR
- DFT-2 allows to analyze further the spectrum

$$\mathrm{var}(\hat v_N) = \frac{PRF^2}{M}\left\{\left[\frac{w_N}{4\sqrt{\pi}}+2w_N^2\frac{S_N}{S_S}+\frac{1}{12}\left(\frac{S_N}{S_S}\right)^2\right]+v_N^2\left[\frac{(S_N-\hat S_N)^2}{\hat S_S^2}\left(\frac{1}{2\sqrt{\pi}w_N}+2\frac{S_N}{S_S}\right)+\left(\frac{S_N}{\hat S_S}\right)^2\right]\right\}$$

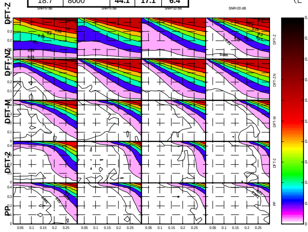

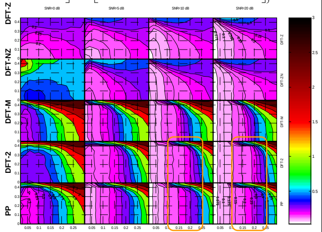

5. 3D Doppler Radar Simulator

ARMAR - 3D Z & V fields

Cartesian Res - Hor: 200m, Ver:60m

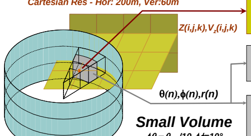

Resolution Volume

54dB IFOV: ∅x:~7200m, Δr:250m

Small Volume

$\Delta\theta = \theta_{3dB}/10$ $\Delta\phi$=10°
$\Delta\rho = \Delta r/3$

- $R=aZ^b$
- $\Lambda = f(R)$ in the DSD expr.
- $v_t(D)=f(D)$ by Atlas
- Mie Scattering

Radial Spectrum $v_r=f(v,v_s,\theta,\phi)$

$W(r_0,r)$

Broadening
- Turbulence
- Wind Shear
- Satellite Motion

Weighted Incoherent Combination

Signal fluct. + thermal noise

Sampling and DFT

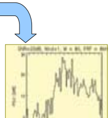

$$w_N = \frac{2}{\lambda PRF}\sqrt{\sigma_R^2+\frac{\theta_{3dB}^2V_S^2}{16\ln(2)}}$$

$$\theta_{3dB} = \alpha\frac{\lambda}{D}$$

$$w_N \approx \frac{5000}{D\cdot PRF}$$

ARMAR and APR-2 3D HiRes fields of reflectivity and Doppler vel. from TOGA/COARE, KWAJEX, CAMEX-3, CAMEX-4 and WAKASA BAY campaigns.

HiRes Cartesian grid:
Δx = 200m (along track)
Δy = 200m (cross-track)
Δz = 60m (vertical)

Spaceborne radar volume of resolution for θ_{3dB} = 0.3°:

IFOV ≅ 2.4 km, Δr ≅ 250m

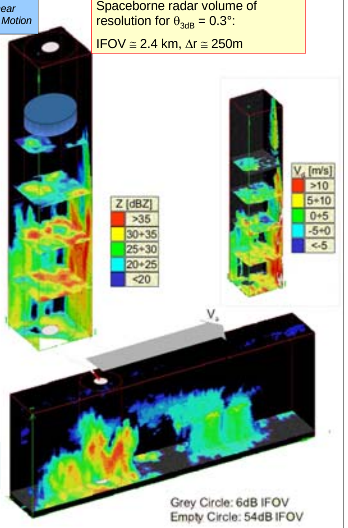

Doppler velocity components

$$v_r = v_P + v_S\,\mathbf{i}_x\cdot(\mathbf{r}-\mathbf{r}_V)/|\mathbf{r}| - \mathbf{u}\cdot\mathbf{r}/|\mathbf{r}|$$

$$v_P \cong v_S\,\mathbf{i}_x\cdot\mathbf{i}_V = v_S\sin(\theta_V)\cos(\phi_V) \cong v_S\cdot x_V'/h_S$$

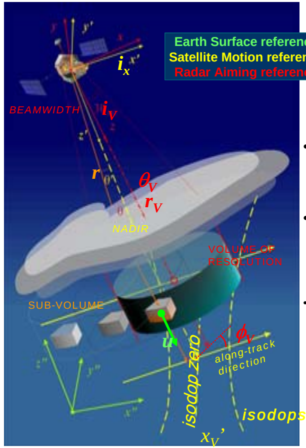

- NUBF (Non Uniform Beam Filling) induces a **bias** on the mean Doppler velocity estimate.
- Using conventional Pair-Pair or FFT techniques, the magnitude of such a bias can be of **several m/s**.
- The bias is highly correlated with the **reflectivity gradient in the along-track direction**. In fact the *isodops* for small θ_{3dB} can be approximated by lines in the cross-track direction.

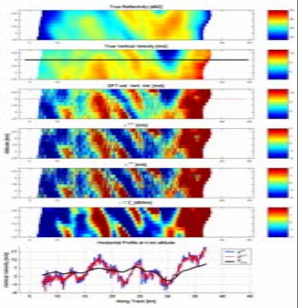

6. Correction of NUBF effects

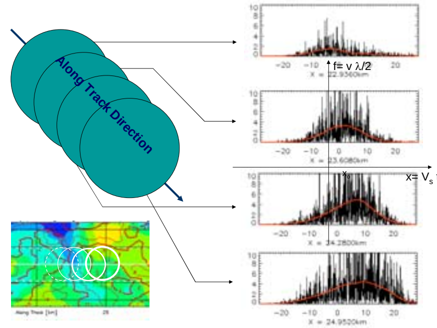

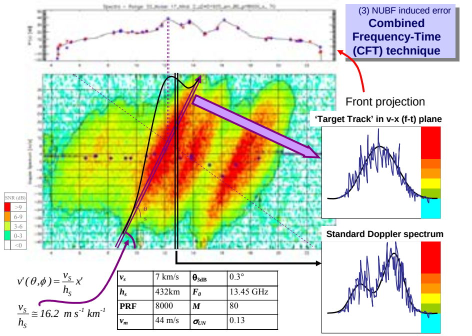

(3) NUBF induced error
Combined Frequency-Time (CFT) technique

$$v'(\theta,\phi) = \frac{v_S}{h_S}x'$$

$$\frac{v_S}{h_S} \cong 16.2\ m\,s^{-1}\,km^{-1}$$

v_s	7 km/s	θ_{3dB}	0.3°
h_s	432km	F_0	13.45 GHz
PRF	8000	M	80
v_m	44 m/s	σ_{UN}	0.13

Spaceborne Simulations

(3) NUBF induced error
ARMAR-KWAJEX case study

ARMAR/CAMEX-3 Hurricane Bonnie

v_s	7 km/s	θ_{3dB}	0.3□
h_s	432km	F_0	13.45 GHz
PRF	6000	M	128

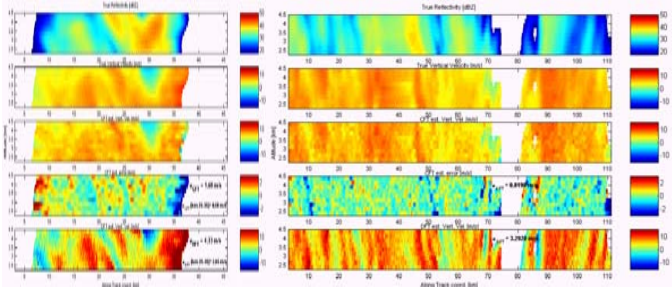

7. Correction of Pointing Errors

(4) Pointing induced error

Effects of Pointing Error

Options to satisfy the scientific requirement of 1 m/s accuracy in vertical rainfall velocity estimates:

1. VERY TIGHT POINTING ACCURACY BUDGET: rms(θ_y) = 4 arcsec is challenging for LEO satellites
2. ANALYSIS OF SEA SURFACE DOPPLER SPECTRUM:
   - Clear air or uniform attenuation field: the measured mean Doppler velocity of the surface corresponds to v_p.
   - NUBF: the sea surface Doppler spectrum is unevenly attenuated and its mean Doppler velocity does not correspond to v_p, in general.

Challenging pointing error budgets

Pointing error (max. θ_y)	Vertical velocity offset (max. $\lvert v_p \rvert$)	
4 arcsec	(λ/270)	⇒ 0.135 m/s
0.01°	(λ/30)	⇒ 1.22 m/s
0.05°	(λ/6)	⇒ 6.1 m/s

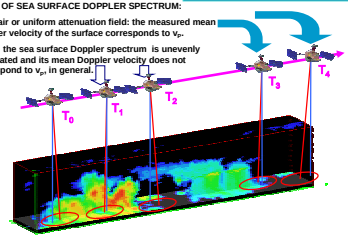

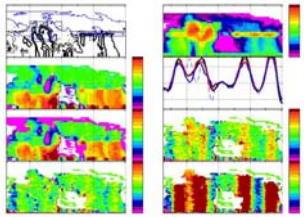

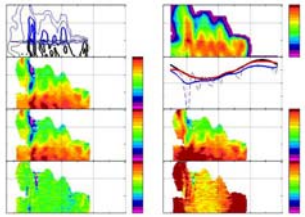

8. Retrieval of Rainfall Parameters

(DFV Bayesian algorithm, Dr. Jonathan Meagher)

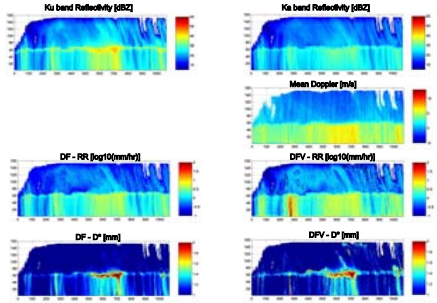

Comparison of Rainfall estimation between dual-frequency (DF) and dual-frequency + Doppler (DFV) Bayesian algorithm.

- DFV produces higher RR and smaller D*
- DFV retrievals show lower retrieval standard deviation especially for low RR and low D*.

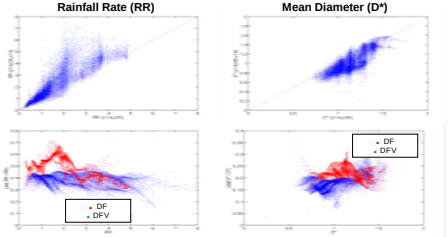

9. Retrieval of Latent Heat profiles

Apparent Heat Source $Q_1 = \frac{\partial \theta}{\partial t} + \nabla \cdot \vec{v}F + \frac{\partial(\theta w)}{\partial z} = Q_R + L_v(\overline{q} - \overline{r}) + (L_s + L_f)(\overline{q} - \overline{s}) + L_f(\overline{r} - \overline{s}) - \nabla \cdot \vec{v}\overline{\theta'} - \frac{\partial \overline{w'\theta'}}{\partial z}$

Hydrometeor Phase Change Rate $P_{12} = \left| \frac{\partial F_1(z)}{\partial z} - \frac{\partial F_2(z)}{\partial z} \right|$

Hydrometeor Vertical Mass Flux $F(z) = M(z)[v_T(z) - w(z)]$

Mean (mass-weighted) Terminal Velocity $v_T = \frac{\pi \rho_l}{6M} \int v_t(D) D^3 N(D) dD$

Mean (reflectivity-weighted) Particle Velocity $v_p = \frac{1}{\eta} \int [v_t(D) - w] \sigma_b(D) N(D) dD$

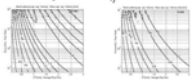

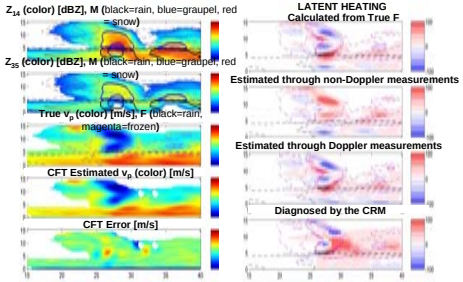

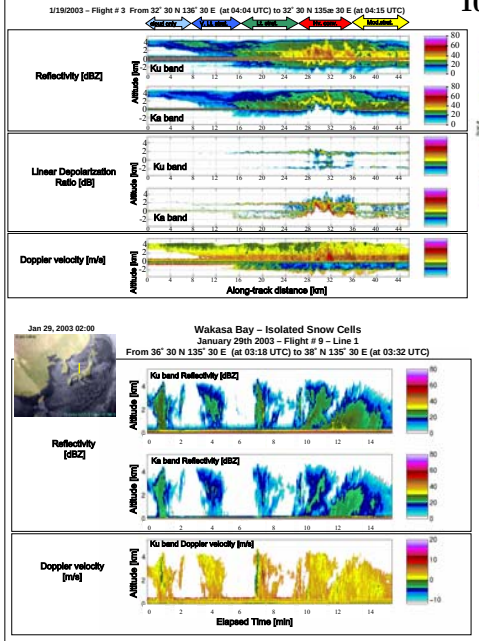

10. Classification of Precipitation (APR-2 Algorithm, S.Tanelli)

Melting Layer Detection - 3D Algorithm Results

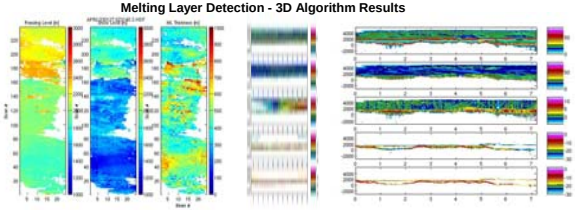

Wakasa Bay – Stratiform rain over ocean (V. Light to Heavy)
January 19th 2003 – Flight #3
From 32° 50' N, 137° 05'E (at 05:42 UTC) to 32° 10' N, 135° 20' E (at 06:04 UTC)

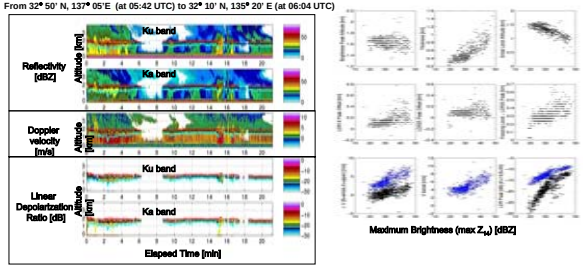

11. Analysis of impact of Multiple Scattering

(Dr. Satoru Kobayashi)

Time-independent analytical model includes effects of multiple scattering as estimated by radiative transfer theory and of backscattering enhancement as well as a finite beam geometry. Incremental reflectivity is relative to single scattering return. Marshall-Palmer DSD, 35 GHz, 100m layer thickness.

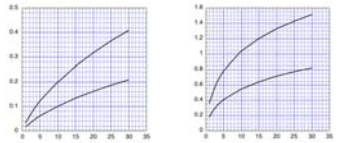

Analytical wave theory (AT) and radiative transfer theory (RT)

Frequency : 95 GH

Diameter : 1mm

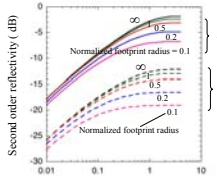

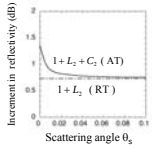

Copolarization

Frequency : 95 GHz

Footprint radius : 22 m

Water spherical particle

Diameter : 1mm

Number density: 5×10^3 m^{-3}
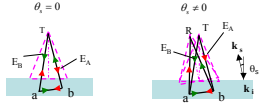
Layer thickness : 100 m